International Journal of Pressure Vessels and Piping 85 (2008) 739–743

Contents lists available at ScienceDirect

International Journal of Pressure Vessels and Piping

journal homepage: www.elsevier.com/locate/ijpvp

Extrapolation of creep life data for 1Cr–0.5Mo steel

B. Wilshire *, P.J. Scharning

Materials Research Centre, School of Engineering, Swansea University, Swansea SA2 8PP, UK

ARTICLE INFO

Article history:
Received 10 December 2007
Received in revised form
31 March 2008
Accepted 3 April 2008

Keywords:
Creep
Creep fracture
Creep life prediction
Ferritic steel

ABSTRACT

A new approach to analysis of stress rupture data allows rationalization, extrapolation and interpretation of multi-batch creep life measurements reported for ferritic 1Cr–0.5Mo tube steel. Specifically, after normalizing the applied stress through the appropriate UTS value, the property sets at various creep temperatures are superimposed onto a sigmoidal 'master curve' using the activation energy for lattice diffusion in the alloy steel matrix (300 kJ mol^{-1}). Despite the considerable batch-to-batch scatter, results from tests lasting less than 30,000 h then allow straightforward prediction of creep lives for stress–temperature conditions causing failure in times up to 150,000 h.

1. Introduction

With large-scale components for steam generation in power stations, design decisions are generally based on the tensile stresses, which the relevant steels can sustain at the operating temperatures without creep failure occurring in 100,000 h [1]. For safe and economic design, many organizations within the EU [2], Japan [3] and the USA [4] have therefore completed large numbers of stress rupture tests lasting up to 100,000 h and more for multiple batches of the various steels chosen for power plant applications.

In addition to responding to the financial and legal requirements of power plant manufacturers and users, the protracted and expensive task of long-term data acquisition has been justified in numerous ways.

(a) The creep rupture properties of power plant steels are characterized by considerable batch-to-batch scatter. Consequently, tests lasting up to 30,000 h are usually completed for at least five melts of each grade [5].
(b) For several newly developed steels, the allowable strengths have been reduced substantially as the maximum test duration has been increased well beyond 30,000 h [6–9]. Moreover, even when considering long-term multi-batch property sets, the estimated strengths depend on the methods selected to make the calculations [6–9], despite the international attention devoted to procedure assessment [2,10].
(c) Data extrapolation would be invalidated by transitions in the processes controlling creep and creep fracture as the test conditions are modified [11,12], i.e. if the dominant mechanism alters, short-term measurements would not allow prediction of long-term performance. Indeed, even without mechanism changes, property extrapolation is complicated by the progressive variations in creep strength as the pre-service microstructures evolve with increasing test duration and temperature.

In contrast to these widely held views, the problems associated with long-term strength estimation may simply reflect the limitations of currently adopted data analysis procedures. For this reason, new relationships have been proposed for rationalization and extrapolation of creep and creep rupture data [13–17]. This methodology has already been shown to allow accurate estimation of 100,000 h strengths from results lasting less than 30,000 h for bainitic 1Cr–1Mo–0.25V rotor forgings [16] and several martensitic 9–12% chromium grades [15,17]. To assess whether this straightforward approach is equally applicable to ferritic materials, the present study considers multi-batch data for 1Cr–0.5Mo tube [18] documented by the National Institute of Materials Science (NIMS), Japan, for test conditions giving creep lives up to about 150,000 h.

2. Experimental results

When determining the allowable design strengths, stress rupture rather than more expensive creep tests are usually performed. So, for 11 batches of 1Cr–0.5Mo tube [18], only 20

* Corresponding author. Tel.: +44 1792 295243; fax: +44 1792 295244.
E-mail address: b.wilshire@swansea.ac.uk (B. Wilshire).

0308-0161/$ - see front matter © 2008 Elsevier Ltd. All rights reserved.
doi:10.1016/j.ijpvp.2008.04.002

values of the minimum creep rate ($\dot{\varepsilon}_m$) were recorded compared with 314 measurements of the time to fracture (t_f). Clearly, the creep life properties showed significant batch-to-batch scatter (Fig. 1). High scatter levels were also found in the values of the UTS (σ_{TS}), and particularly the 0.2% proof stress (σ_{PS}) determined from high-strain-rate tensile tests ($\sim 10^{-3}\,s^{-1}$) at room temperature to 650 °C for each batch of steel investigated (Fig. 2).

Although relatively few creep tests were carried out [18], t_f increases as $\dot{\varepsilon}_m$ decreases (Fig. 3), verifying that the creep life is governed by the rate of creep strain accumulation. In line with standard practice, the dependences of $\dot{\varepsilon}_m$ and t_f on stress (σ) and temperature (T) were then described [18] using power law expressions of the form

$$M/t_f = \dot{\varepsilon}_m = A\sigma^n \exp(-Q_c/RT) \tag{1}$$

where $R = 8.314\,J\,mol^{-1}\,K^{-1}$. Even so, M ($=\dot{\varepsilon}_m t_f$) decreases from ~0.03 towards ~0.01 as t_f increases from around 30,000 to 150,000 h (Fig. 3), while the parameter (A), the stress exponent (n) and the apparent activation energy for creep (Q_c) also vary as the test conditions change. Thus, a decrease from $n \cong 14$ to 3 occurs as the test duration and temperature increase (Fig. 1), with Q_c ranging from around 490 to 280 kJ mol^{-1}.

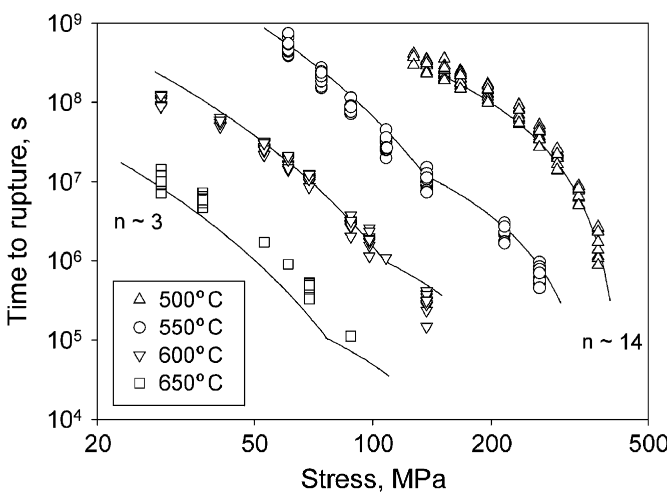

Fig. 1. The stress dependence of the creep life for 1Cr–0.5Mo steel at 500–650 °C, comparing the measured values [18] with the predictions based on Eq. (4) shown as solid lines.

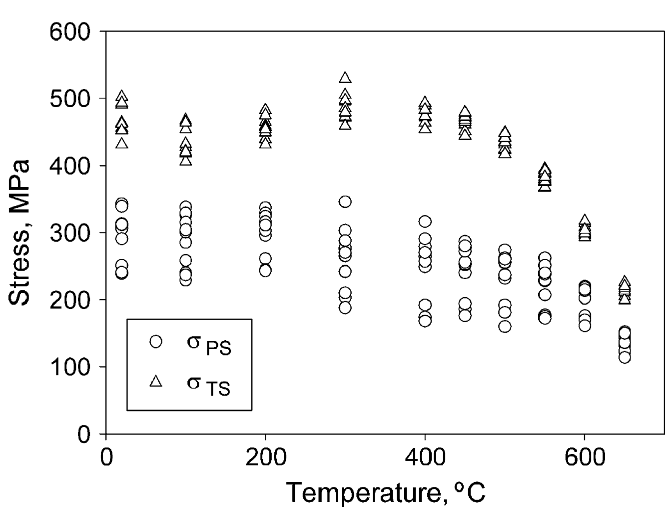

Fig. 2. The variations of the 0.2% proof stress (σ_{PS}) and the ultimate tensile stress (σ_{TS}) with temperature for multiple batches of 1Cr–0.5Mo tube steels [18].

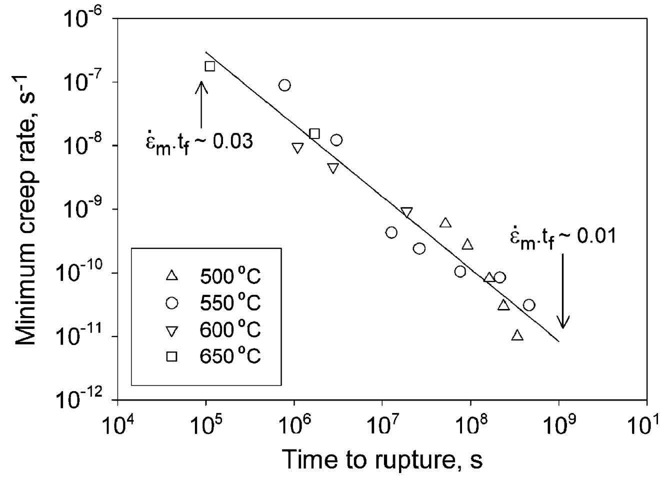

Fig. 3. The dependence of the creep life on the minimum creep rate for 1Cr–0.5Mo steel at 500–650 °C [18].

2.1. Parametric approaches to data analysis

The unpredictable variations in n and Q_c mean that long-term design strengths cannot be obtained reliably using Eq. (1) to extrapolate short-term measurements. Instead, the NIMS approach [19] has been to adopt various parametric relationships [20–22], defining time–temperature parameters, which can be plotted as functions of stress to superimpose multi-batch data onto 'master curves' for a given steel. However, no single parametric method has proved capable of fitting the experimental data for the majority of the many power plant steels characterised by NIMS and, even when the best fitting procedure is selected, the accuracies achieved are not always satisfactory [19].

The NIMS results for the 1Cr–0.5Mo tube samples (Fig. 1) were processed using the Manson–Haferd parameter (P_{MH}), given by [21]

$$P_{MH} = \frac{\log t_f - \log t_a}{T - T_a} \tag{2}$$

with the numerical values of t_a and T_a estimated by curvilinear regression [18]. This approach superimposes the stress rupture properties (Fig. 4), but the scatter combined with the unknown curvature of parametric plots makes even limited data extrapolation unreliable. Moreover, the unusual gradient changes in the Manson–Haferd curve require a satisfactory explanation.

2.2. Rationalization of stress rupture data

As an alternative to empirical parametric procedures, the t_f values recorded for several power plant steels have been effectively superimposed onto 'master curves' simply by normalizing σ through the σ_{TS} value at the creep temperature for each batch of steel [15–17]. In this way, Eq. (1) becomes

$$M/t_f = \dot{\varepsilon}_m = A^*(\sigma/\sigma_{TS})^n \exp(-Q_c^*/RT) \tag{3}$$

where $A^* \neq A$ and $Q_c^* \neq Q_c$. With Eq. (3), Q_c^* is obtained from the temperature dependences of $\dot{\varepsilon}_m$ and t_f at constant σ/σ_{TS}, whereas Q_c is calculated at constant σ with Eq. (1).

Using Eq. (3), together with the appropriate NIMS σ_{TS} values in Fig. 2, the results presented in Fig. 1 are superimposed in Fig. 5. For the ferritic 1Cr–0.5Mo steel, as reported for bainitic 1Cr–1Mo–0.25V [16] and martensitic 9–12% chromium grades [15,17], $Q_c^* \cong 300$ kJ mol^{-1}, a value close to the activation energy for lattice diffusion in the alloy steel matrices. Interestingly, rationalization of the multi-batch t_f measurements using Eq. (3)

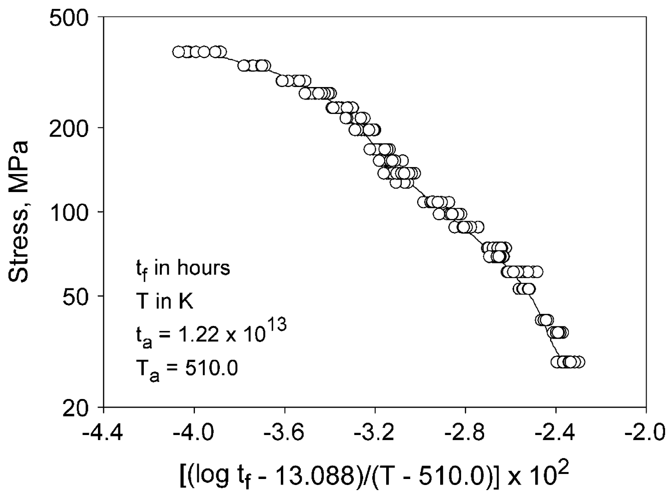

Fig. 4. Superimposition of the multi-batch stress rupture measurements reported for 1Cr–0.5Mo steel [18], using the Manson–Haferd relationship [21].

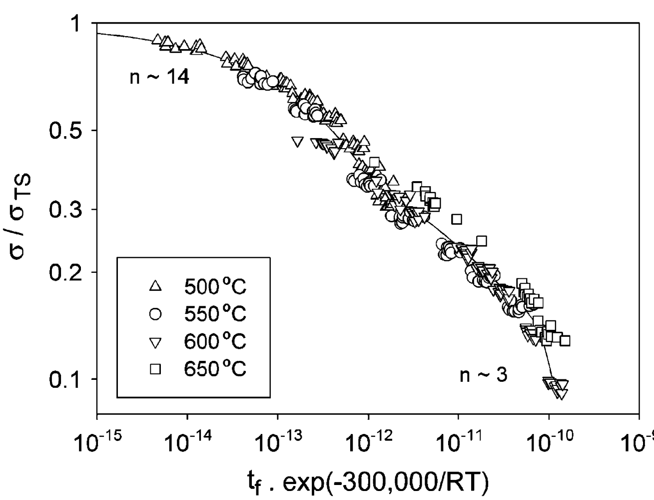

Fig. 5. The dependence of the temperature-compensated creep life on the normalized stress (σ/σ_{TS}) for 1Cr–0.5Mo steel, using Eq. (3) with $Q_c^* = 300\,\text{kJ mol}^{-1}$.

reproduces the unusual shape of the Manson–Haferd curve (Fig. 4).

In addition to superimposing the t_f results, Eq. (3) avoids the large and variable Q_c values derived using Eq. (1), but does not eliminate the decrease from $n \cong 14$ to 3 as (σ/σ_{TS}) is reduced (Fig. 5). This unpredictable fall in n value then means that Eq. (3) also fails to allow reliable estimation of long-term stress rupture properties by extrapolation of short-term t_f values. For this reason, a new methodology has been introduced [13–17], building on the property rationalization achieved by normalizing σ through σ_{TS} (Fig. 5).

2.3. Extrapolation of stress rupture data

Obviously, σ_{TS} defines the maximum stress, which can be applied at the creep temperature, so property sets can be described over the full stress range from $(\sigma/\sigma_{TS}) = 1$ to $(\sigma/\sigma_{TS}) = 0$. Successful time/temperature relationships must then make it evident that $t_f \to 0$ when $(\sigma/\sigma_{TS}) \to 1$, with points of inflection in the stress rupture curves ensuring that $t_f \to \infty$ when $(\sigma/\sigma_{TS}) \to 0$. This form of curve is obtained by quantifying the stress and temperature dependences of t_f as

$$(\sigma/\sigma_{TS}) = \exp\{-k_1[t_f \exp(-Q_c^*/RT)]^u\} \quad (4)$$

where k_1 and u are easily evaluated [13–17] from plots of $\ln[t_f \exp(-Q_c^*/RT)]$ against $\ln[-\ln(\sigma/\sigma_{TS})]$. Adopting this procedure, again $Q_c^* = 300\,\text{kJ mol}^{-1}$, while analysis of t_f measurements for tests lasting less than 30,000 h reveals a gradient change, such that k_1 and u differ in the high and low (σ/σ_{TS}) regimes for the 1Cr–0.5Mo tube samples (Fig. 6). In fact, by considering the values of σ_{PS} as well as σ_{TS}, it appears that this change in k_1 and u occurs when the applied stress is reduced from above to below about $0.8\sigma_{PS}$ (Fig. 6).

Eq. (4) is inherently stable on extrapolation so, knowing the (σ/σ_{TS}) ranges within which the different k_1 and u values apply (Fig. 6), t_f can be computed over extended stress ranges at selected temperatures. These predictions fit well with the long-term NIMS data for 1Cr–0.5Mo steel at 500, 550 and 600 °C, but are less impressive at the highest test temperature of 650 °C (Fig. 1).

Knowing k_1 and u in the high and low (σ/σ_{TS}) regimes, Eq. (4) also allows the t_f measurements for all stress/temperature combinations causing failure in times up to 150,000 h to be superimposed onto the sigmoidal 'master curve' presented in Fig. 7. Alternatively, using only the k_1 and u values for the high (σ/σ_{TS}) range, the predicted creep lives progressively underestimate the actual t_f measurements as σ is reduced below about $0.4\sigma_{TS}$ (Fig. 7). In this way, Eq. (4) provides an unambiguous method for identification of the short-term t_f values, which should not be included in extrapolation exercises undertaken to estimate long-term creep rupture strengths. In addition, with decreasing applied stress, it is clear that the measured long-term creep lives increasingly exceed the property trends expected from the high-stress data (Fig. 7), accounting for the unusual gradient changes in the Manson–Haferd curve (Fig. 4) and the rationalized power law plot (Fig. 5).

3. Discussion

The results presented in Figs. 6 and 7 are of interest in relation to three different types of behaviour pattern reported when Eq. (4) was applied to data sets obtained for other materials [13–17].

(a) With the martensitic 9–12% chromium steels, Grades 92 and 122 [17], as well as bainitic 1Cr–1Mo–0.25V rotor steel [16],

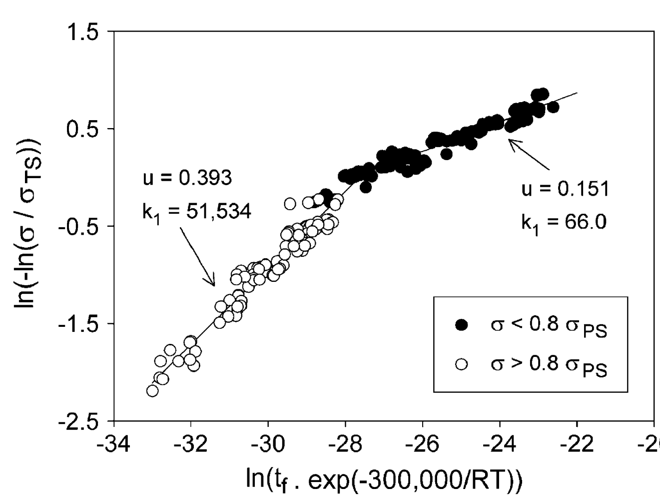

Fig. 6. The dependence of the temperature-compensated creep life on $\ln[-\ln(\sigma/\sigma_{TS})]$ for 1Cr–0.5Mo steel at 500–650 °C, applying Eq. (4) with $Q_c^* = 300\,\text{kJ mol}^{-1}$ to test results with creep lives less than 30,000 h.

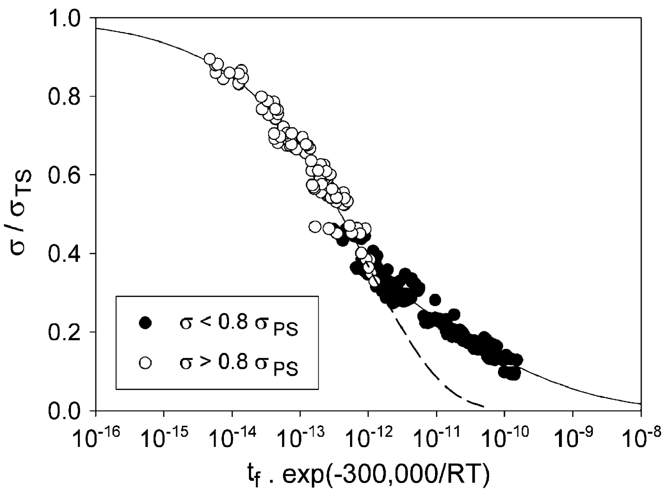

Fig. 7. The dependence of the temperature-compensated creep life on the normalized stress (σ/σ_{TS}) for 1Cr–0.5Mo steel at 500–650 °C, showing the predictions based on Eq. (4) with $Q_c^* = 300\,\mathrm{kJ\,mol^{-1}}$, together with creep life measurements from tests lasting up to about 150,000 h. The solid line was determined by recognizing the change in k_1 and u as (σ/σ_{TS}) decreased in Fig. 6, while the broken line illustrates the underestimation of long-term creep rupture properties determined experimentally when only the k_1 and u values from the high (σ/σ_{TS}) range are incorporated into Eq. (4).

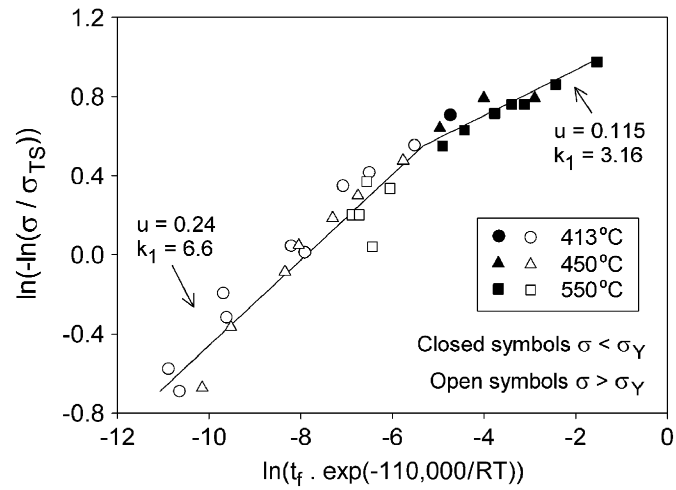

Fig. 8. Evaluation of the coefficients in Eq. (4) by plotting $\ln[t_f \exp(-110{,}000/RT)]$ against $\ln[-\ln(\sigma/\sigma_{TS})]$ for polycrystalline copper at 413–550 °C [13], distinguishing between tests carried out at stresses above and below the yield stress, σ_Y (shown as open and closed symbols, respectively).

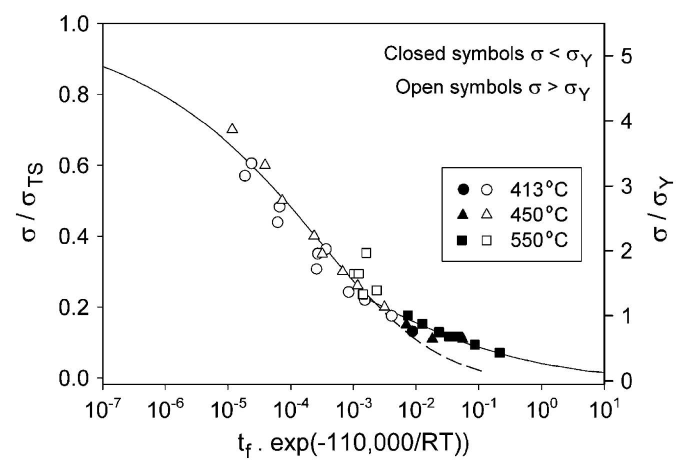

Fig. 9. The dependences of $\log[t_f \exp(-110{,}000/RT)]$ on (σ/σ_{TS}) and (σ/σ_Y) for polycrystalline copper at 413–550 °C, distinguishing between tests carried out when (σ/σ_Y) >1 (open symbols) and (σ/σ_Y)<1 (closed symbols). The predictions based on Eq. (4) using the k_1 and u values in Fig. 8 are shown as solid lines, while the broken line indicates the underestimation of the low stress properties when k_1 and u from only the high (σ/σ_{TS}) range are incorporated into Eq. (4) [13].

analysis of results with t_f<30,000 h accurately predicted the multi-batch 100,000 h rupture strengths, with k_1 and u differing in the high and low (σ/σ_{TS}) regimes. However, in contrast to the present observations for 1Cr–0.5Mo tube samples, extrapolation exercises based only on the k_1 and u values in the high (σ/σ_{TS}) range overestimated rather than underestimated actual long-term performance. Even so, this effect was not a consequence of a distinctive transition in creep or creep fracture mechanism. Instead, the changes in k_1 and u were linked to differences in the rates of creep strength reduction caused by microstructure evolution with increasing test duration and temperature. This interpretation was supported by the observation that a significant fall in the hardness of fractured testpieces occurred only when $t_f \exp(-300{,}000/RT)$ increased in the low (σ/σ_{TS}) range [16,17].

(b) With the martensitic 9% chromium steel, Grade 91 [17], and the commercial aluminium alloy, 2124 [14], no changes in k_1 and u were found for t_f measurements from tests lasting less than 30,000 h. Yet, the derived k_1 and u values allowed accurate prediction of t_f data for stress–temperature conditions giving creep lives up to 100,000 h. With the Grade 91 steel, it again appears that the creep strength falls as the martensitic microstructure evolves during creep exposure but, in this case, the hardness of fractured specimens decreased continuously as $t_f \exp(-300{,}000/RT)$ increased [17].

(c) Behaviour similar to that now observed for 1Cr–0.5Mo tube (Figs. 6 and 7) has been found previously [13] for pure polycrystalline copper (Figs. 8 and 9). With copper, on adopting Eq. (4), k_1 and u differ in the high and low (σ/σ_{TS}) ranges, depending whether $\sigma > \sigma_Y$ or $\sigma < \sigma_Y$ (Fig. 8), where σ_Y is the yield stress determined from high-strain-rate tensile tests at the creep temperature. Using the k_1 and u values for the appropriate (σ/σ_{TS}) regimes then accurately describes the stress rupture properties over the entire range of test conditions covered. Moreover, incorporating k_1 and u only for the high (σ/σ_{TS}) levels into Eq. (4) underestimates the long-term creep lives (Fig. 9), in line with the results now obtained for 1Cr–0.5Mo steel (Fig. 7).

In the investigation undertaken for copper [13], the stress and temperature dependences of $\dot{\varepsilon}_m$ and t_f were discussed in relation to evidence derived from microstructural studies, stress change experiments and the different patterns of creep strain accumulation as the test conditions were varied. This information established that, when the initial loading strains are essentially elastic under stresses such that $\sigma < \sigma_Y$, the recorded $\dot{\varepsilon}_m$ values are much lower than the rates predicted from measurements made in the high σ/σ_Y range when rapid dislocation multiplication produces a plastic component of the initial strain on loading [13]. Because t_f increases as $\dot{\varepsilon}_m$ decreases, as (σ/σ_{TS}) is reduced, the measured creep lives when $\sigma < \sigma_Y$ progressively exceed the t_f values predicted by extrapolation of the property trends identified when $\sigma > \sigma_Y$ (Fig. 9).

While the change in k_1 and u occurred when σ decreased from above to below σ_Y with copper (Fig. 8), although the scatter in σ_{PS} values is high (Fig. 2), k_1 and u differ when σ is reduced from above to below about 0.8 σ_{PS} with 1Cr–0.5Mo tube samples (Fig. 6). Clearly, σ_{PS} must be slightly greater than σ_Y, with the similarities in the behaviour patterns in Figs. 6 and 7 and in Figs. 8 and 9 suggesting that $\sigma_Y \cong 0.8\ \sigma_{PS}$ for 1Cr–0.5Mo tube. On this basis, the deformation and damage processes governing the creep and creep fracture properties appear to be essentially the same for polycrystalline copper [13] and for ferritic 1Cr–0.5Mo steel.

4. Conclusions

The multi-batch creep rupture properties of 1Cr–0.5Mo tube steel are superimposed onto a sigmoidal 'master curve' by describing the stress and temperature dependences of the creep lives as

$$(\sigma/\sigma_{TS}) = \exp\{-k_1[t_f\ \exp(-Q_c^*/RT)]^u\}$$

where σ_{TS} is the UTS at the creep temperature for each batch of steel investigated, while Q_c^* ($= 300\,\mathrm{kJ\,mol^{-1}}$) is the activation energy for matrix diffusion. The coefficients (k_1 and u) are easily evaluated, but differ in the high and low (σ/σ_{TS}) regimes, changing when σ falls from above to below about $0.8\sigma_{PS}$, where σ_{PS} is the 0.2% proof stress at the relevant creep temperature. Even so, knowing the (σ/σ_{TS}) ranges within which the different k_1 and u values apply, analyses of t_f measurements from tests lasting less than 30,000 h allow straightforward prediction of stress rupture data determined for times up to 150,000 h.

The behaviour patterns observed for ferritic 1Cr–0.5Mo steel are also shown to be comparable with the stress rupture properties displayed by polycrystalline copper rather than the creep life characteristics observed for several other power plant steels, such as bainitic 1Cr–1Mo–0.25V forgings and martensitic 9–12% chromium grades.

Acknowledgements

The authors gratefully acknowledge the financial support for the Materials Centre of Excellence in Technology and Industrial Collaboration (CETIC) provided by the Welsh Assembly Government.

References

[1] 'ASME boiler and pressure vessel code', Section II, Part D, Appendix I. New York: ASME; 2004. p. 789.
[2] Merckling G. Long term creep rupture strength assessment: the development of the European Collaborative Creep Committee post assessment tests. In: Shibli IA, Holdsworth SR, Merckling G, editors. Proceedings of ECCC international conference on 'creep and fracture in high temperature components—design and life assessment issues'. London: DEStech Publ; 2005. p. 3–19.
[3] Yagi K. Acquisition of long-term creep data and knowledge for new applications. In: Shibli IA, Holdsworth SR, Merckling G, editors. Proceedings of ECCC international conference on 'creep and fracture in high temperature components—design and life assessment issues'. London: DEStech Publ; 2005. p. 31–45.
[4] Viswanathan R, Henry JF, Tanzosh J, Stanko G, Shingledecker J. US program on materials technology for ultrasupercritical coal power plants. In: Shibli IA, Holdsworth SR, Merckling G, editors. Proceedings of ECCC international conference on 'creep and fracture in high temperature components—design and life assessment issues'. London: DEStech Publ; 2005. p. 59–74.
[5] Hald J. Creep strength and ductility of 9 to 12% chromium steels. Mater High Temp 2004;41:41–6.
[6] Bendick W, Gabrel J. Assessment of creep rupture strength for the new martensitic 9% Cr steels E911 and T/P 92. In: Shibli IA, Holdsworth SR, Merckling G, editors. Proceedings of ECCC international conference on 'creep and fracture in high temperature components—design and life assessment issues'. London: DEStech Publ; 2005. p. 406–18.
[7] Kimura K. Review of allowable stress and new guideline of long-term creep strength assessment for high Cr ferritic creep resistant steels. In: Shibli IA, Holdsworth SR, Merckling G, editors. Proceedings of ECCC international conference on 'creep and fracture in high temperature components—design and life assessment issues'. London: DEStech Publ; 2005. p. 1009–22.
[8] Cipolla L, Gabrel J. New creep rupture assessment of Grade 91. In: Proceedings of the first international conference on 'super-high strength steels'. AIM, Rome, CD-Rom; 2005.
[9] Di Gianfrancesco A, Cipolla L, Cirilli F, Cumino G, Caminada S. Microstructural stability and creep data assessment of Tenaris Grades 91 and 911. In: Proceedings of the first international conference on 'super-high strength steels'. AIM, Rome, CD-Rom; 2005.
[10] Holdsworth SR, Askins M, Baker A, Gariboldi E, Holmstrom S, Klenk A, et al. Factors influencing creep model equation selection. In: Shibli IA, Holdsworth SR, Merckling G, editors. Proceedings of ECCC international conference on 'creep and fracture in high temperature components—design and life assessment issues'. London: DEStech Publ; 2005. p. 380–93.
[11] Ennis PJ. The significance of microstructural changes and steam oxidation for the service life of chromium steel components. In: Shibli IA, Holdsworth SR, Merckling G, editors. Proceedings of ECCC international conference on 'creep and fracture in high temperature components—design and life assessment issues'. London: DEStech Publ; 2005. p. 279–87.
[12] Maruyama K, Lee JS. Causes of overestimation of creep rupture strengths in 11Cr–2W–0.3Mo–CuVNb steel. In: Shibli IA, Holdsworth SR, Merckling G, editors. Proceedings of ECCC international conference on 'creep and fracture in high temperature components—design and life assessment issues'. London: DEStech Publ; 2005. p. 372–9.
[13] Wilshire B, Battenbough AJ. Creep and creep fracture of polycrystalline copper. Mater Sci Eng A 2007;443A:156–66.
[14] Wilshire B, Burt H, Lavery N. Prediction of long-term stress-rupture data for 2124. Mater Sci Forum 2006;519–521:1041–6.
[15] Wilshire B, Scharning PJ. Creep ductilities of 9–12% chromium steels. Scripta Mater 2007;56:1023–6.
[16] Wilshire B, Scharning PJ. Prediction of long-term creep data for forged 1Cr–1Mo–0.25V steel. Mater Sci Technol 2008;24:1–9.
[17] Wilshire B, Scharning PJ. A new methodology for analysis of creep and creep fracture data for 9–12% chromium steels. Inter Mater Rev 2008;53: 91–104.
[18] NIMS Creep Data Sheet No. 1B. Data sheets on the elevated temperature properties of 1Cr–0.5Mo steel tubes for boilers and heat exchangers, 1996.
[19] Kimura K. Present status and future prospect of NIMS creep data sheet. In: Mishra RS, Earthman JC, Raj SV, Viswanathan R, editors. Creep deformation and fracture, design and life extension. Pittsburg: MS&T; 2005. p. 97–106.
[20] Larson FR, Miller J. A time-dependent relationship for rupture and creep stresses. Trans ASME 1952;74:765–75.
[21] Manson SS, Haferd AM. A linear time–temperature relationship for extrapolation of creep and stress rupture data. TN: NASA; 1953. 2890.
[22] Orr RL, Sherby OD, Dorn JE. Correlations of rupture data for metals at elevated temperatures. Trans ASM 1954;46:113–28.